NANO LETTERS

2004
Vol. 4, No. 11
2065−2071

Mechanical Shuttling of Linear Motor-Molecules in Condensed Phases on Solid Substrates

Tony Jun Huang,[†,⊥] Hsian-Rong Tseng,[‡,||] Lin Sha,[§] Weixing Lu,[†,⊥] Branden Brough,[†,⊥] Amar H. Flood,[‡,||] Bi-Dan Yu,[†,⊥] Paul C. Celestre,[‡,||] Jane P. Chang,[§] J. Fraser Stoddart,*[,‡,||,⊥] and Chih-Ming Ho*[,†,||,⊥]

Mechanical and Aerospace Engineering Department, Department of Chemistry and Biochemistry, Chemical Engineering Department, California NanoSystems Institute, Institute for Cell Mimetic Space Exploration, University of California, Los Angeles, Los Angeles, California 90095

Received November 28, 2003; Revised Manuscript Received June 1, 2004

ABSTRACT

From analyses of pressure–area isotherms and X-ray photoelectron spectra, we have demonstrated that redox-controllable molecular shuttles, in the shape of amphiphilic, bistable rotaxanes, are mechanically switchable in closely packed Langmuir films with chemical reagents. Additionally, mechanical switching has been proven to occur in closely packed Langmuir–Blodgett bilayers while mounted on solid substrates. The results not only constitute a proof of principle but they also provide the impetus to develop solid-state nanoelectromechanical systems that have the potential to reach up to the mesoscale.

Although motor-molecules are known[1,2] to be commonplace in living systems, the construction of artificial molecular-level machines was only a glint in the eyes of a physicist[3] and a few followers until recent times.[4] Employing the concepts of self-assembly and molecular recognition, chemists have begun to apply template-directed protocols[5] to the synthesis of a family of mechanically interlocked molecules called[6] rotaxanes. In their simplest manifestation, rotaxanes are composed of mutually recognizable and intercommunicating ring and dumbbell-shaped components. Like an abacus, relative linear motion is introduced into a rotaxane when the ring component moves back and forth spontaneously and degenerately between two identical recognition sites (or stations), located symmetrically along the rod section of the dumbbell-shaped component. Such a rotaxane has been referred to (Scheme 1A) as a molecular shuttle.[7] Controllable molecular shuttles (Scheme 1B), wherein the ring component can be induced to move on command by some appropriate stimulus between two nonidentical stations, constituted the next significant advance[8] in linear motor-molecule design using rotaxanes. Such controllable molecular shuttles, which can be driven chemically,[9] electrochemically,[10] and photochemically[11] in solution, have been recognized[12−14] as integral components in the development of functioning nanosystems for nanotechnology. In particular, the mechanical movements operating in these motor-molecules are yet to be realized as the nanoactuating materials in, for example, nanoelectromechanical systems (NEMS).

Scheme 1. (A) Schematic Representation of a Degenerate, Thermally Activated Molecular Shuttle. (B) Schematic Representation of a Non-degenerate, Redox-controllable Molecular Shuttle

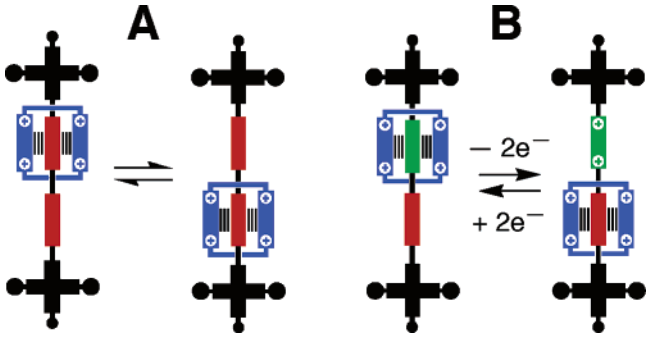

Rotaxanes form a class of wholly synthetic motor-molecules with a range of properties that make them ideally suited as nanoactuators. Switchable rotaxanes can be acti-

* Corresponding authors. Fraser Stoddart, Department of Chemistry and Biochemistry, 405 Hilgard Avenue, Los Angeles, CA 90095; Phone (310) 206-7078; Fax (310) 206-1843; E-mail stoddart@chem.ucla.edu. Chih-Ming Ho, Mechanical and Aerospace Engineering Department, 420 Westwood Plaza, Los Angeles, CA 90095; Phone (310) 825-9993; Fax (310) 206-2302; E-mail: chihming@seas.ucla.edu.

[†] Mechanical and Aerospace Engineering Department.
[‡] Department of Chemistry and Biochemistry.
[§] Chemical Engineering Department.
[||] California NanoSystems Institute.
[⊥] Institute for Cell Mimetic Space Exploration.

10.1021/nl035099x CCC: $27.50
Published on Web 10/13/2004

vated by multiple stimuli (vide supra), a situation that cannot be reproduced using biomotors, which rely on chemical energy alone.[1,2] Rotaxanes can be constructed in a modular manner[4] by integrating different components, an approach which allows them to be optimized and customized. These two characteristics allow a design flexibility[15,16] that is desirable for a multitude of engineering applications. Bistability is unique to these particular "all-or-nothing" rotaxanes, wherein the motor-molecule exists to all intents and purposes in only one of two states. Moreover, the motor-molecules are metastable,[17] i.e., they persist in their switched state for a period of time (aproximately seconds, at room temperature) after the stimulus has been removed. Consequently, these motor-molecules do not need a continuous input of energy for maintaining the system in each state and, coupled with the already low energy cost[18] of switching, e.g., ~1 eV, the metastability provides an attractive feature for NEMS applications. Rough estimates[19] have indicated that the mechanical force generated by a single bistable rotaxane switching process could be as large as 100 pN, i.e., an order of magnitude greater than the force produced by biomotors, such as kinesin and myosin.[1,2] With these advantages in mind, we have become interested in developing rotaxane-based mechanical devices, using the force and movement generated by the molecular switching process.

The relative linear motions of the moving components in a large number of controllable molecular shuttle molecules distributed randomly in the solution state cannot be expressed coherently in a mechanical context. And so it becomes imperative to self-organize these nanoscale machines at interfaces[11b,17,20] in order to bring coherence and cooperativity to bear upon their coordinated performance in the macroscopic world. However, before any rotaxane-based NEMS devices become viable for real applications, their mechanical switching must be shown to operate when the molecules are mounted in closely packed monolayers on solid supports. This demonstration has been the central theme of this investigation and is the prime focus of this letter.

Here we report the results of four different experiments involving two constitutionally isomeric, amphiphilic, bistable rotaxanes. In the first experiment, evidence that one of the two redox-controllable rotaxanes exhibits markedly different surface pressure−mean area (π-A) isotherm curves, depending on whether an oxidant is present or absent in the subphase of the Langmuir trough at the beginning of the experiment, is presented. The fact that, in a control experiment, the corresponding dumbbell compound, i.e., the rotaxane minus the ring, does not reveal any π-A dependence on its redox state implies that mechanical motion most likely occurs between the dumbbell and ring components of the rotaxane, depending on its redox state. In a second round of experiments, also carried out with Langmuir films of the same compounds on an aqueous subphase, the oxidant was introduced at two different surface pressures (10 and 30 mN m^{-1}) after compression of the monolayer was well underway. These experiments suggest that the redox-driven movements of the rotaxane's components can be initiated even when the molecules are highly pressurized in the monolayer. In a third type of experiment, redox-switching of two amphiphilic bistable rotaxanes in highly pressurized Langmuir films has been demonstrated yet more directly by transferring them onto solid supports and locating the relative positions of the rings on the dumbbells by X-ray photoelectron spectroscopy (XPS). Quantitative spectroscopic analyses establish that the ring moves completely from one station to the other. Finally, in a fourth and final experiment, the same kinds of relative mechanical motions have also been observed by XPS in the outer water-penetratable layer of an LB double layer on a solid support when it is immersed in an aqueous solution of the oxidant, namely, $Fe(ClO_4)_3$. Since most mechanical systems rely on solid media to transmit actuation forces, the results in this communication not only constitute a proof of principle but they also provide the impetus to go on and develop molecular shuttle-based chemomechanical systems at the nanoscale level.

Scheme 2. Structural Formulas and Idealized Graphical Representations of the Rotaxane $\mathbf{1}^{4+}$ and Other Compounds (Dumbbell **2** of $\mathbf{1}^{4+}$ and the Constitutionally Isomeric Rotaxane $\mathbf{3}^{4+}$ and Its Dumbbell **4**) Used in the Control Experiments[a]

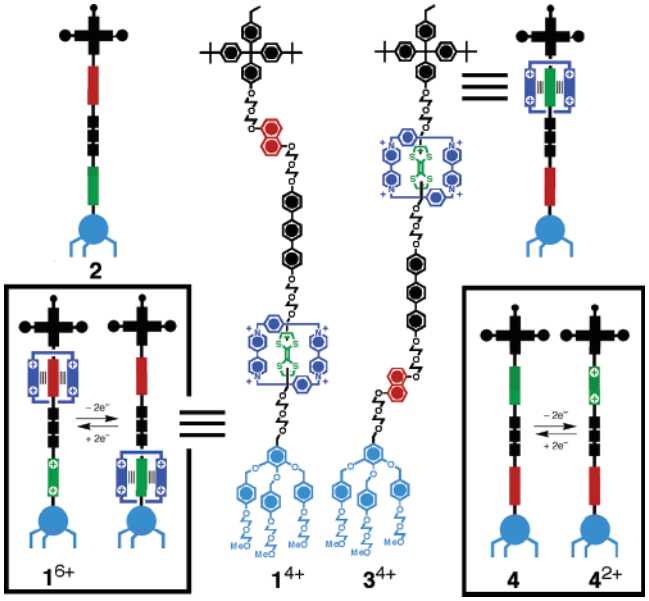

[a] Graphical representations of the oxidative switching in the rotaxane $\mathbf{1}^{4+}$, leading to mechanical movement of the ring , and in the dumbbell **4**, are illustrated. Note that $\mathbf{1}^{4+}$ and $\mathbf{3}^{4+}$ have been employed as their $4PF_6^-$ salts in all the redox experiments reported in this communication. Oxidative switching was achieved with aqueous solutions containing 10^{-3} or 10^{-4} M $Fe(ClO_4)_3$.

The structural formula and graphical representation of the rotaxane $\mathbf{1}^{4+}$ are shown in Scheme 2. The molecule consists of a tetracationic ring component (dark blue) and a linear rod section that contains two different stations, a tetrathiafulvalene (TTF) unit (green) and a dioxynaphthalene (DNP) unit (red), separated by a rigid terphenylene spacer (black). A hydrophilic (light blue) and a hydrophobic (black) stopper are incorporated at each end of the rod, enabling the molecules to form LB films. The starting state $\mathbf{1}^{4+}$ of this bistable rotaxane has its TTF unit encircled by the tetracationic ring. Upon oxidation, the TTF unit becomes dicationic (TTF^{2+}) and experiences Coulombic repulsion with

the tetracationic ring, causing the ring to shuttle toward the DNP unit in the oxidized state $\mathbf{1}^{6+}$. Conversely, reduction of the TTF^{2+} dication in $\mathbf{1}^{6+}$ back to a neutral TTF unit causes the rotaxane to return to its starting state $\mathbf{1}^{4+}$. Thus, this rotaxane, with these two reversibly switchable redox states involving ring translation, can be likened to a linear motor. Scheme 2 also shows the structural formulas and graphical presentations of other compounds, the dumbbell **2** of $\mathbf{1}^{4+}$ and the constitutionally isomeric rotaxane $\mathbf{3}^{4+}$ and its dumbbell **4**, used in the control experiments. The difference between $\mathbf{1}^{4+}$ and $\mathbf{3}^{4+}$ relates only to the relative positioning of the TTF and DNP residues with respect to the two different stoppers. The dumbbells **2** and **4** are both neutral compounds in which the rings have been removed from the rotaxanes $\mathbf{1}^{4+}$ and $\mathbf{3}^{4+}$, respectively.[21]

Evidence for the switching of the rotaxane $\mathbf{1}^{4+}$ was first observed with highly packed Langmuir films in a $\pi-A$ isotherm analysis.[22] The oxidized rotaxane $\mathbf{1}^{6+}$ was obtained by premixing the oxidant $Fe(ClO_4)_3$ into the aqueous subphase at a concentration of 10^{-4} M. After spreading the rotaxane $\mathbf{1}^{4+}$ solution onto the subphase, the oxidant was allowed to diffuse, during a 1-hour period, to the air−liquid interface where it presumably oxidized the neutral TTF unit to its dicationic (TTF^{2+}) form which, in turn, induced the tetracationic ring to move to the DNP unit. Figure 1A shows that there are significant differences between the isotherms for the starting state ($\mathbf{1}^{4+}$) and oxidized ($\mathbf{1}^{6+}$) molecules, although both display the classic phase transformations from a gas phase through a liquid-expanded one and then onto a liquid-condensed phase. For most regions along the $\pi-A$ isotherm, the oxidized rotaxane $\mathbf{1}^{6+}$ appears to occupy more area than its starting-state counterpart $\mathbf{1}^{4+}$ under the same pressure. The two curves also display different phase transformation characteristics. For $\mathbf{1}^{4+}$, the transition region between liquid-expanded and liquid-condensed phases starts at 31 mN m^{-1} and ends at 35 mN m^{-1}, while, for $\mathbf{1}^{6+}$ it starts at 20 mN m^{-1} and ends at 24 mN m^{-1}. Control experiments were conducted with the dumbbell **2**. Figure 1B shows that the isotherm curves of the oxidized dumbbell $\mathbf{2}^{2+}$ and its starting state **2** are practically identical, a finding which suggests[23] that the isotherm curve difference between $\mathbf{1}^{4+}$ and $\mathbf{1}^{6+}$ might be caused by the ring component moving along the dumbbell component from one (TTF) recognition site to the other (DNP). The reason for exercising caution in interpreting these results stems from at least two considerations: (i) we are looking at a multiparameter system and (ii) we are comparing like with like when we relate a neutral dumbbell compound being oxidized to a charged (dicationic) species to an already charged (tetracationic) rotaxane being oxidized to a more highly charged (hexcationic) species. These considerations beg two further questions: what is the role of hydration in the monolayers, and, are there counterions present in the monolayers, and if so, which − PF_6^- and/or ClO_4^-? In a search for an answer to the first question,

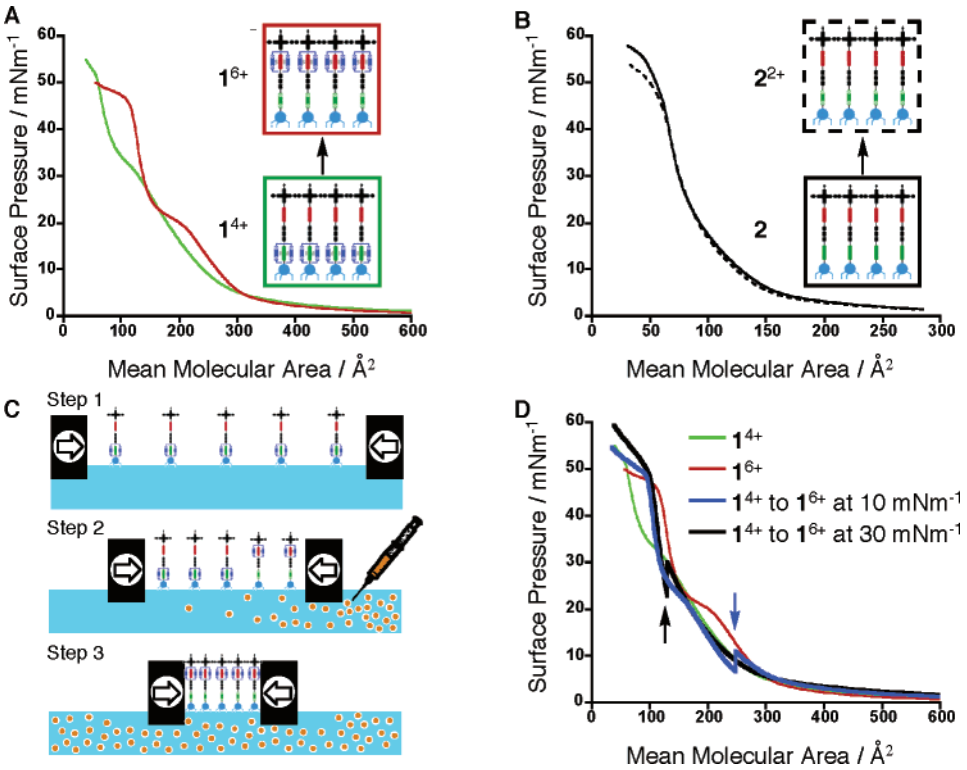

Figure 1. Surface pressure versus mean area isotherm curves for: (A) the starting-state rotaxane $\mathbf{1}^{4+}$ and $\mathbf{1}^{6+}$, oxidized by $Fe(ClO_4)_3$ in the aqueous subphase during spreading of the monolayer; (B) the starting-state dumbbell **2** and $\mathbf{2}^{2+}$ oxidized by $Fe(ClO_4)_3$ in the aqueous subphase during spreading of the monolayer. (C) Schematic representation of steps 1, 2, and 3 in the experimental procedure employed to switch (step 3) the rotaxane molecules $\mathbf{1}^{4+}$ to their oxidized counterpart $\mathbf{1}^{6+}$ after compressing (step 1) the rotaxane monolayers and injecting (step 2) the oxidant $Fe(ClO_4)_3$ into the subphase at pressures of 10 and 30 mN m^{-1} in separate experiments. (D) Surface pressure versus mean area isotherm curves for the starting state rotaxane $\mathbf{1}^{4+}$ oxidized by $Fe(ClO_4)_3$ in highly packed Langmuir films at both 10 and 30 mN m^{-1} compared to the isotherms for $\mathbf{1}^{4+}$ and $\mathbf{1}^{6+}$ shown previously in (A).

on-the-trough Langmuir monolayers of not-too-dissimilar amphiphilic, bistable [2]rotaxanes, characterized using X-ray reflectance measurements, have been found[24] to exist in folded ground-state conformations which, upon exposure to the oxidant [$Fe(ClO_4)_3$] in the subphase, the rotaxane unfolds and the Langmuir film absorbs a large number (~50) of water molecules. An answer to the second question comes from the observation that reflection absorption IR spectroscopy (RAIRS) of seven LB layers of $\mathbf{1}^{4+}$ and its oxidized form $\mathbf{1}^{6+}$, both transferred onto a gold substrate, reveal a number of significant changes in the intensities of vibrational bands associated with counterions. The most noteworthy difference is the complete absence of the PF_6^- bands present at 850 and 560 cm^{-1} in the multiple layers of $\mathbf{1}^{4+}$ and the appearance, in their place in the seven LB layers of $\mathbf{1}^{6+}$, of ClO_4^- bands at 1100 and 630 cm^{-1}, respectively. These observations testify to the complete exchange of PF_6^- anions present in the $\mathbf{1}^{4+}$ Langmuir monolayer for ClO_4^- anions, which were introduced into the subphase with the oxidant used to effect the oxidation of $\mathbf{1}^{4+}$ to $\mathbf{1}^{6+}$, prior to the latter being produced as a Langmuir monolayer.

To demonstrate that the rotaxane $\mathbf{1}^{4+}$ retains the features in the isotherm, which suggests that mechanical switching is operating in a highly packed film, the rotaxane monolayers were compressed (step 1 in Figure 1C) with pauses introduced at different pressures, specifically at 10 and 30 mN m^{-1}. Initially, these isotherms showed the same behavior as the previously recorded isotherms (Figure 1A) for the starting-state rotaxane $\mathbf{1}^{4+}$. Oxidant was injected (step 2 in Figure 1C) into the subphase during the pauses, and an hour was allowed to pass in order to give the oxidant time to diffuse to the surface and initiate the switching of the molecules within the monolayer. In the meantime, the pressure dropped as a result of molecular relaxation. When pressurization was continued (step 3 in Figure 1C), the isotherm curves displayed characteristics similar to those in the isotherms previously observed for switched molecules, i.e., $\mathbf{1}^{6+}$. This observation suggests that, in highly pressurized and ordered Langmuir films, the rotaxane molecules are still able to switch in a manner identical to that already witnessed in the unpressurized state.

We will now present evidence for the redox-controlled mechanical switching of the rotaxanes within highly packed Langmuir films using XPS on account of the fact that there could be more than one interpretation of the isotherm results. We first carried out XPS measurements[25] on LB films of both amphiphilic, bistable rotaxanes ($\mathbf{1}^{4+}$ and $\mathbf{3}^{4+}$) and their respective dumbbells (**2** and **4**). The photoemission intensity of each element depends on the depth at which the photoelectron is emitted and it attenuates exponentially with increased depth. Therefore, the XPS technique can be used to differentiate atoms at different depths within a film. The XPS signal intensity ($I_{A,Z}$) for a layer of atoms (A) buried at a distance Z underneath the film surface can be expressed[26] as

$$I_{A,Z} = I_A^0 \exp\left(\frac{-Z}{\lambda(E_A)\sin\theta}\right) \quad (1)$$

where $I^0{}_A$ represents the signal intensity obtained from a layer of atoms located at the film surface, $\lambda(E_A)$ is the photoelectron attenuation length of A, which is a function of the kinetic energy of the emitted photoelectrons, and θ is the takeoff angle, which equals 90° in the present investigation. Thus, the photoemission intensity from a layer of atoms A embedded closer to the surface (smaller Z) will be stronger than that arising from a layer of the same atoms buried deeper (larger Z) in the film.

Molecular shuttling can be monitored[27] by using XPS to track nitrogen (N), which is present solely in the bistable rotaxane's only moving part, the ring component. Langmuir monolayers were prepared[26] for both the starting states ($\mathbf{1}^{4+}$ and $\mathbf{3}^{4+}$) and the oxidized rotaxanes ($\mathbf{1}^{6+}$ and $\mathbf{3}^{6+}$), along with their dumbbell counterparts **2** and **4**, and $\mathbf{2}^{2+}$ and $\mathbf{4}^{2+}$, respectively. Next, monolayers were transferred to substrates[28] as LB films for XPS analysis. Figure 2A shows the N 1s photoemission spectra of $\mathbf{1}^{4+}$ and $\mathbf{1}^{6+}$, along with those of **2** and $\mathbf{2}^{2+}$. There is no nitrogen signal observed for the ringless dumbbell compounds, confirming that the peaks revealed in the $\mathbf{1}^{4+}$ and $\mathbf{1}^{6+}$ spectra are from the N atoms in the ring. Furthermore, a higher intensity for the N 1s peak is observed in the oxidized rotaxane $\mathbf{1}^{6+}$ film than in the starting state, an observation which supports the hypothesis that, in the oxidized rotaxane, the ring encircles the DNP recognition site and not the TTF^{2+} site, placing it closer to the film's surface. Control experiments were conducted using the rotaxane $\mathbf{3}^{4+}$ in which the positions of the TTF and DNP sites are the reverse of those in $\mathbf{1}^{4+}$. Figure 2B shows clearly that the N 1s photoemission intensity was higher in the case of the starting-state rotaxane $\mathbf{3}^{4+}$ in which the ring encircles the TTF site, i.e., the one closer to the film's surface. These control experiments ruled out the possibility of an oxidation-induced change in the N density as well as the influence of the rotaxanes unfolding, and demonstrated the capability of XPS to track the movement of the rings in LB films of redox-controllable rotaxanes.

Molecules of $\mathbf{1}^{4+}$ were switched in situ in highly packed Langmuir monolayers (Figure 1C, steps 1−3) and transferred to substrates for XPS analysis. Once again, a much higher intensity of the N 1s peak is observed (Figure 2C) for the molecules switched in situ within highly packed Langmuir monolayers than that observed for the starting state of the bistable rotaxane. Furthermore, the line shape and intensity of the N 1s peak remain similar to those recorded (Figure 2A) for the oxidized molecule $\mathbf{1}^{6+}$. These data prove that bistable rotaxanes (Scheme 2) are mechanically switchable in closely packed Langmuir films.

To establish that the ring moves completely from one station to the other while the molecules are in closely packed Langmuir films, the distance traveled by the ring component in the switchable rotaxane was quantified using XPS. The first step in the quantitative analysis was to determine the average attenuation length of Si 2p photoelectrons in Langmuir films by measuring the attenuated Si 2p intensities at different rotaxane layer thicknesses, which were measured by ellipsometry.[29] When the logarithms of the Si 2p intensities were plotted as a function of the film's thickness,

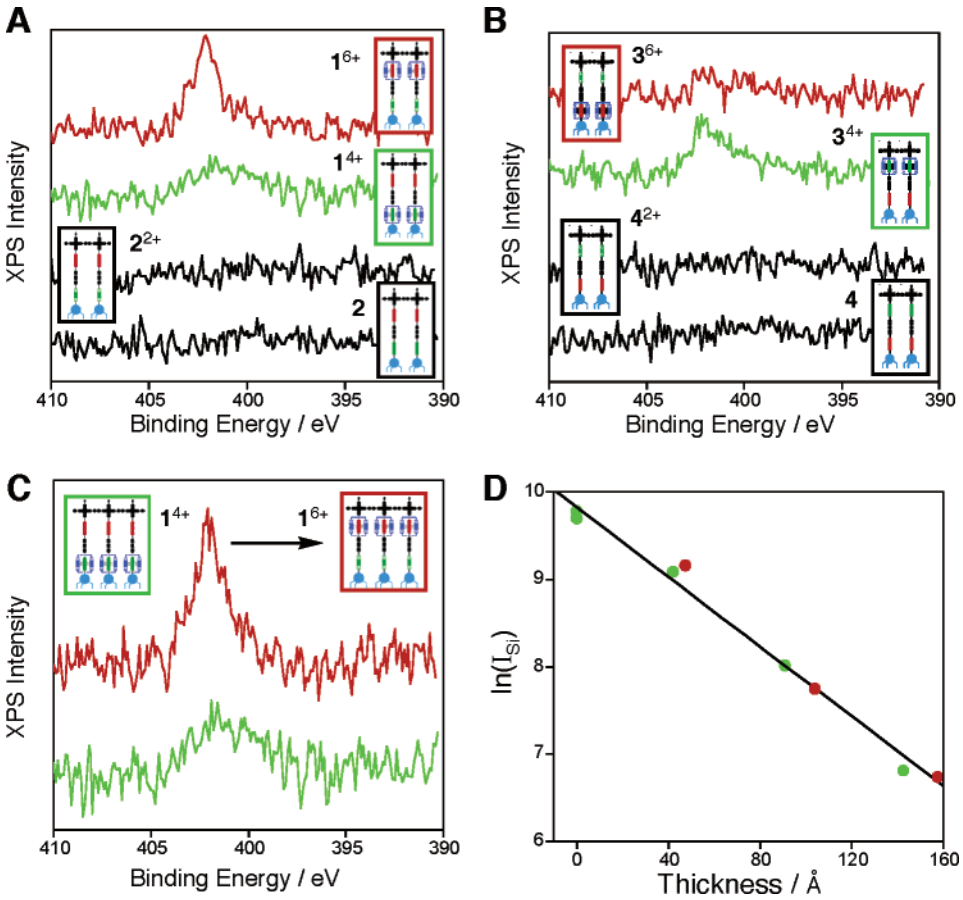

Figure 2. Nitrogen 1s X-ray photoemission spectra for: (A) the starting-state rotaxane $\mathbf{1}^{4+}$ (green line) and its oxidized form $\mathbf{1}^{6+}$ (red line) and their respective dumbbells **2** (black line) and $\mathbf{2}^{2+}$ (black line); (B) the starting-state rotaxane $\mathbf{3}^{4+}$ (green line) and its oxidized form $\mathbf{3}^{6+}$ (red line) and their respective dumbbells **4** (black line) and $\mathbf{4}^{2+}$ (black line); (C) the rotaxane $\mathbf{1}^{6+}$ (red line) having been switched (oxidized) in a highly packed monolayer compared with its starting-state $\mathbf{1}^{4+}$ (green line). (D) Logarithms of Si 2p photoemission intensities versus film thickness measured by ellipsometry. The red dots represent samples composed of oxidized rotaxane molecules $\mathbf{1}^{6+}$, and the green dots represent samples composed of the starting-state molecules $\mathbf{1}^{4+}$.

a linear relationship was observed (Figure 2D). From eq 1, the photoelectron attenuation length of Si 2p electrons in Langmuir films was calculated to be about 5.0 nm, since the slope of this linear regression line is $-1/\lambda(E_{Si})$. The photoelectron attenuation length for the N 1s electrons was then calculated to be about 4.1 nm, based on the power-law dependence[25] of attenuation lengths on the kinetic energies of photoelectrons:

$$\frac{\lambda(E_N)}{\lambda(E_{Si})} = \left(\frac{E_N}{E_{Si}}\right)^{0.79} \quad (2)$$

Note that E_N and E_{Si} are the kinetic energies of photoelectrons emitted from the N 1s and Si 2p orbitals, and that they are equal to about 1084 and 1386 eV, respectively, assuming a work function of 3 to 5 eV. The calculated attenuation lengths agreed well with the literature which reports[30] inelastic mean free paths of 2.5 to 4.2 nm for polymers and some organic materials at an electron energy of ~1000 eV. Finally, Figure 2D displays measurements from both switched (red dots) and starting-state (green dots) samples. Both data sets were fitted to one linear regression line, confirming that the photoelectron attenuation length does not change during the molecular switching process. Thus, we can calculate the distance traveled (ΔZ) by the ring in the direction perpendicular to the substrate's surface.

$$\Delta Z = Z_{\text{starting-state}} - Z_{\text{switched}} = \lambda(E_N) \times \ln(I_{N,\text{switched}}/I_{N,\text{starting-state}}) \quad (3)$$

A value of 1.9 nm for the distance traveled along the Z direction was determined from the data shown in Figure 2B. Molecular modeling[31] indicates that the distance of the ring shuttling along the fully stretched 8.0 nm length of the rotaxane $\mathbf{1}^{4+}$ molecule is 3.7 nm, i.e., 46% of the total molecular length. Since the film's thickness was found to be only 4.4 nm by ellipsometry, the translational value of 1.9 nm, namely, 42% of the film's total thickness, is in good agreement with the modeling result.

To turn a rotaxane-based NEMS device into an engineering reality, we must prove that these mechanically interlocked molecules maintain their shuttling properties while mounted on a solid substrate as closely packed films. Therefore, the investigation was extended into the realm of LB films themselves. LB double layers of the starting-state rotaxane $\mathbf{3}^{4+}$ molecules were deposited on a silicon dioxide substrate at a

surface pressure of 25 mN m^{-1}, and the N 1s photoemission intensity was measured by XPS. The substrate, coated with the LB double layers, was then immersed in a solution containing the oxidant[32] and probed again by XPS. A double layer, instead of a single layer, was chosen because the exposed surfaces of double-layer samples are hydrophilic (as opposed to the hydrophobic nature of a single layer), allowing the oxidant in the aqueous solution to penetrate the surface and oxidize the TTF unit. It is expected that only molecules in the top layer will be oxidized and switched. Thus, we attribute the observed difference (Figure 3) in the two N 1s spectra to mechanical switching, as characterized by ring movements that occur within the outermost layer of the film, even when the molecules are attached to a solid substrate.

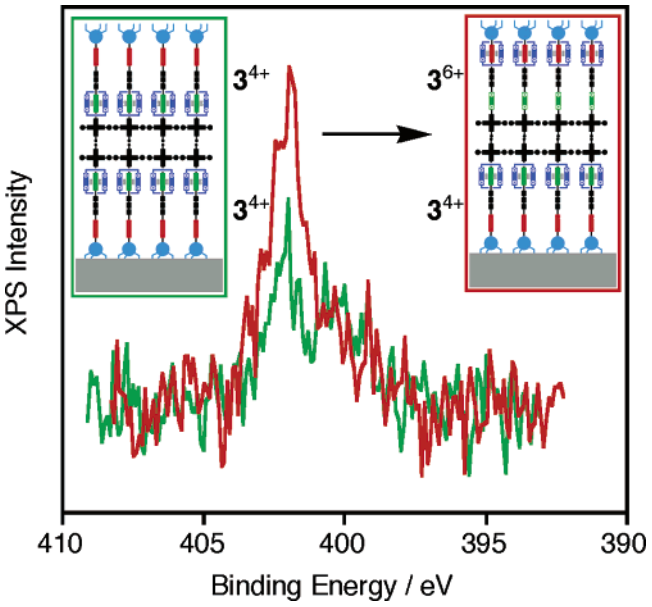

Figure 3. Nitrogen 1s photoemission spectra for the rotaxane $\mathbf{3}^{4+}$ in LB double layers prior to (green line) and after (red line) immersing samples into an aqueous solution of $Fe(ClO_4)_3$.

In summary, quantitative XPS analysis has proven that the ring component of a bistable amphiphilic [2]rotaxane can be switched completely from one station to the other along the dumbbell component in self-organized, closely packed Langmuir monolayers. Moreover, XPS analysis also indicates that the mechanical operation of these linear motor-molecules is maintained, even when they are closely packed within Langmuir−Blodgett films mounted on solid supports. Our long-term objective is to develop motor-molecule-activated mechanical systems, using the force and movement generated by the molecular switching process. The research reported in this communication marks a substantial step toward that objective. We believe that, by integrating a bottom-up approach based on self-assembly and self-organization of motor-molecules with a top-down approach based on micro/nanofabrication, a new class of functioning nano- and mesoscale mechanical and optical devices could become a reality in the not-too-distant future.

Acknowledgment. The authors appreciate the help from Dr. Tzung-Fang Guo and Professor Yang Yang for obtaining RAIRS data. The authors acknowledge support of this work by the Defense Advanced Projects Research Agency (DARPA) Biomolecular Motors program and a National Science Foundation NIRT grant (ECS-0103559).

Supporting Information Available: Reflection absorption IR spectra of 7-layer Langmuir−Blodgett films; UV−visible-NIR transmission spectra of Langmuir−Blodgett multilayers. This material is available free of charge via the Internet at http://pubs.acs.org.

References

(1) Goodsell, D. S. *Our Molecular Nature: The Body's Motors, Machines, and Messages*; Copernicus: New York, 1996.
(2) Boyer, P. D. *J. Biol. Chem.* **2002**, *277*, 39045−39061.
(3) Feynman, R. P. *Eng. Sci.* **1960**, *23*, 22−36.
(4) (a) Balzani, V.; Credi, A.; Raymo, F. M.; Stoddart, J. F. *Angew. Chem., Int. Ed.* **2000**, *39*, 3348−3391. (b) Balzani, V.; Credi, A.; Venturi, M. *Molecular Devices and Machines − A Journal into the Nanoworld*; Wiley-VCH: Weinheim, 2003.
(5) (a) Anderson, S.; Anderson, H. L.; Sanders, J. K. M. *Acc. Chem. Res.* **1993**, *26*, 469−475. (b) Hoss, R.; Vögtle, F. *Angew. Chem., Int. Ed. Engl.* **1994**, *33*, 375−384. (c) Hubin, T. J.; Busch, D. L. *Coord. Chem. Rev.* **2000**, *200−202*, 5−52. (d) Stoddart, J. F.; Tseng, H.-R. *Proc. Natl. Acad. Sci. U.S.A.* **2002**, *99*, 4797−4800.
(6) (a) Schill, G. *Catenanes, Rotaxanes, and Knots*; Academic Press: New York, 1971. (b) Sauvage, J.-P.; Dietrich-Buchecker, C., Eds. *Molecular Catenanes, Rotaxanes and Knots*; Wiley-VCH: Weinheim, 1999.
(7) Anelli, P.-L.; Spencer, N.; Stoddart, J. F. *J. Am. Chem. Soc.* **1991**, *113*, 5131−5133.
(8) (a) Bissell, R. A.; Córdova, E.; Kaifer, A. E.; Stoddart, J. F. *Nature* **1994**, *369*, 133−137. (b) Anelli, P.-L.; Asakawa, M.; Ashton, P. R.; Bissell, R. A.; Clavier, G.; Gorski, R.; Kaifer, A. E.; Langford, S. J.; Mattersteig, G.; Menzer, S.; Philp, D.; Slawin, A. M. Z.; Spencer, N.; Stoddart, J. F.; Tolley, M. S.; Williams, D. J. *Chem. Eur. J.* **1997**, *3*, 1113−1135.
(9) (a) Martínez-Díaz, M.-V.; Spencer, N.; Stoddart, J. F. *Angew. Chem., Int. Ed. Engl.* **1997**, *36*, 1904−1907. (b) Kelly, T. R.; De Silva, H.; Silva, R. A. *Nature* **1999**, *401*, 150−152. (c) Elizarov, A. M.; Chiu, S.-H.; Stoddart, J. F. *J. Org. Chem.* **2002**, *67*, 9175−9181.
(10) (a) Raehm, L.; Kern, J. M.; Sauvage, J.-P. *Chem. Eur. J.* **1999**, *5*, 3310−3317. (b) Gaviña, P.; Sauvage, J.-P. *Tetrahedron Lett.* **1997**, *38*, 3521−3524. (c) Armaroli, N.; Balzani, V.; Collin, J.-P.; Gaviña, P.; Sauvage, J.-P. *J. Am. Chem. Soc.* **1999**, *121*, 4397−4408.
(11) (a) Brouwer, A. M.; Frochot, C.; Gatti, F. G.; Leigh, D. A.; Mottier, L.; Paolucci, F.; Roffia, S.; Wurpel, G. W. H. *Science* **2001**, *291*, 2124−2128. (b) Feringa, B. L.; Koumara, N.; van Delden, R. A.; Ter Wiel, M. K. J. *Appl. Phys. A* **2002**, *75*, 301−308. (c) Blanco, M.-J.; Jiménez, M. C.; Chambron, J.-C.; Heitz, V.; Linke, M.; Sauvage, J.-P. *Chem. Soc. Rev.* **1999**, *28*, 293−305. (d) Mulder, A.; Jukovic, A.; Lucas, L. N.; van Esch, J.; Feringa, B. L.; Huskens, J.; Reinhoudt, D. N. *Chem. Commun.* **2002**, 2734−2735.
(12) (a) Stoddart, J. F. *Chem. Aust.* **1992**, *59*, 576−577 and 581. (b) Preece, J. A.; Stoddart, J. F. *Nanobiology* **1994**, *3*, 149−166. (c) Gómez-López, M.; Preece, J. A.; Stoddart, J. F. *Nanotechnology* **1996**, *7*, 183−92. (d) Colasson, B. X.; Dietrich-Buchecker, C.; Jimenez-Molero, M. C.; Sauvage, J.-P. *J. Phys. Org. Chem.* **2002**, *15*, 476−483.
(13) (a) Collier, C. P.; Wong, E. W.; Belohradsky, M.; Raymo, F. M.; Stoddart, J. F.; Kuekes, P. J.; Williams, R. S.; Heath, J. R. *Science* **1999**, *285*, 391−394. (b) Diehl, M. R.; Steuerman, D. W.; Tseng, H.-R.; Vignon, S. A.; Celestre, P. C.; Stoddart, J. F.; Heath, J. R. *ChemPhysChem* **2003**, *4*, 1335−1339.
(14) Luo, Y.; Collier, C. P.; Jeppesen, J. O.; Nielsen, K. A.; DeIonno, E.; Ho, G.; Perkins, J.; Tseng, H. R.; Yamamoto, T.; Stoddart, J. F.; Heath, J. R. *ChemPhysChem* **2002**, *3*, 519−525.
(15) Tseng, H. R.; Vignon, S. A.; Stoddart, J. F. *Angew. Chem., Int. Ed.* **2003**, *42*, 1491−1495.
(16) (a) Chia, S. Y.; Cao, J. G.; Stoddart, J. F.; Zink, J. I. *Angew. Chem., Int. Ed.* **2001**, *40*, 2447−2451. (b) Kim, K.; Jeon, W. S.; Kang, J.-K.; Lee, J. W.; Jon, S. Y.; Kim, Y.; Kim, K. *Angew. Chem., Int. Ed.* **2003**, *42*, 2293−2296. (c) Hernandez, R.; Tseng, H.-R., Wong, J. W.; Stoddart, J. F.; Zink, J. I. *J. Am. Chem. Soc.* **2004**, *126*, 3370−3371.

(17) Tseng, H.-R.; Wu, D.; Fang, N.; Zhang, X.; Stoddart, J. F. *ChemPhysChem* **2004**, *5*, 111−116.
(18) Estimate based on the voltage required to electrochemically switch catenanes based on TTF and $CBPQT^{4+}$ components. See: Balzani, V.; Credi, A.; Mattersteig, G.; Matthews, O. A.; Raymo, F. M.; Stoddart, J. F.; Venturi, M.; White, A. J. P.; Williams, D. J. *J. Org. Chem.* **2000**, *65*, 1924−1936.
(19) Molecular force estimates were calculated using Coulombic repulsion assuming a 1 nm diameter ring carrying four evenly dispersed positive charges which is encircling a site containing two positive charges. Movement is assumed to proceed linearly, 3.7 nm away from the starting position.
(20) (a) Raehm, L.; Kern, J.-M.; Sauvage, J.-P.; Hamann, C.; Palacin, S.; Bourgoin, J.-P. *Eur. J. Org. Chem.* **2002**, *8*, 2153-2162. (b) Hou, S.; Sagara, T.; Xu, D.; Kelly, T. R.; Gamz, E. *Nanotechnology* **2003**, *14*, 566−570.
(21) The synthesis of **1**·$4PF_6$, **2**, **3**·$4PF_6$, **4** have been reported recently in a full paper. See: Tseng, H.-R.; Vignon, S. A.; Celestre, P. C.; Perkins, J.; Jeppesen, J. O.; Di Fabio, A.; Ballardini, R.; Gandolfi, M. T.; Venturi, M.; Balzani, V.; Stoddart, J. F. *Chem. Eur. J.* **2003**, *9*, 155−172.
(22) Langmuir films were fabricated and isotherms were analyzed using a KSV alternate trough system. After spreading a $CHCl_3$ solution of the amphiphilic compound, the solvent is allowed to evaporate, leaving a molecular monolayer at the air−water interface consisting solely of the rotaxane or dumbbell molecules. The $CHCl_3$ used in these experiments was stored over basic alumina and distilled immediately prior to use. For the starting-state molecules, i.e., the rotaxanes $\mathbf{1}^{4+}$ and $\mathbf{3}^{4+}$, and their dumbbell counterparts **2** and **4**, respectively, deionized water (18.2 MΩ) was used as the subphase. The compression speed that was used for all the rotaxane and dumbbell films was 2 $Å^2$/molecule-min. All isotherms, which were obtained for starting-state and oxidized molecules, were highly reproducible.
(23) A comparison of the $\pi-A$ isotherms of the rotaxane $\mathbf{1}^{4+}$ and its dumbbell component **2** reveals that the rotaxane occupies approximately twice the mean molecular area. For example, at 20 mN m^{-1}, the rotaxane fills an area of ∼1.75 nm^2, whereas the dumbbell occupies an area of only ∼0.90 nm^2. These data are consistent with results (Lee, I. C.; Frank, C. W.; Yamamoto, T.; Tseng, H.-R.; Flood, A. H.; Stoddart, J. F.; Jeppesen, J. O. *Langmuir* **2004**, *20*, 5809−5828) which suggest that, at pressures below the transition region, the rotaxane exists in a folded conformation, whereas, under similar conditions, the dumbbell is unfolded.
(24) Nϕrgaard, K.; Jeppesen, J. O.; Laursen, B. O.; Simonsen, J. B.; Weygand, M. J.; Kjaer, K.; Stoddart, J. F.; Bjϕrholm, T. Submitted.
(25) The XPS data were obtained on a VG ESCALAB 5 electron spectrometer using Al Ka X-ray radiation (1486.6 eV) with a pass-energy of 20 eV at a takeoff angle of 90° (normal to the film surface). The photoemission of surface carbon (C 1s) at 284.6 eV was used as the reference binding energy. The weak photoemission intensity of N 1s is a consequence of the low nitrogen atomic density (less than 1 at. %), which approaches the XPS detection limit.
(26) (a) Chang, J. P.; Green, M. L.; Donnelly, V. M.; Opila, R. L.; Eng, J., Jr.; Sapjeta, J.; Silverman, P. J.; Weir, B.; Lu, H. C.; Gustafsson, T.; Garfunkel, E. *J. Appl. Phys.* **2000**, 87, 4449−4455. (b) Woodruff, D. P.; Delchar, T. A. *Modern Techniques of Surface Science*; Cambridge University: London 1994.
(27) Molecular shuttling can also be monitored by spectroscopic methods. Hence, UV−visible-NIR transmission spectroscopy of multiples (8, 16, 24, 32) of LB monolayers transferred to quartz slides display the characteristic charge-transfer bands associated with the tetracationic ring's location in the starting state. Specifically, $\mathbf{1}^{4+}$ shows a weak red-shifted band at 930 nm that doubles in intensity between 16 and 32 layers, while $\mathbf{1}^{6+}$ shows a similarly weak and red-shifted band at 550 nm that displays a linear correlation of intensity with the number of layers. These observations lend qualitative support to the redox-controlled mechanical switching of the amphiphilic bistable rotaxanes in Langmuir films.
(28) All monolayers were transferred to hydrophilic silicon dioxide substrates at a surface pressure of 25 mN m^{-1} as LB films. Prior to monolayer depositions, the silicon dioxide substrates were prepared as follows: (i) Piranha (H_2SO_4/H_2O_2 = 5:1) cleaning for 5 min, (ii) deionized water cleaning for 5 min, and (iii) air-drying.
(29) Film thickness measurements were performed using a Gaertner L116B ellipsometer with an index of refraction of 1.46.
(30) Compton, P. J. *Surf. Interface Anal.* **2001**, *31*, 23−34.
(31) Molecular modeling was performed in *ChemBats3D* by extending the molecule fully and then optimizing with the MM2 force field to obtain "correct" bond lengths and angles. The distance was measured from the center of the TTF unit to the center of the DNP unit. This fully extended conformation, which is employed for convenience in the graphical representations, does not reflect the variety of folded conformations that these compounds may realistically occupy in solution or in Langmuir and LB monolayers.
(32) The oxidant solution was prepared by mixing $Fe(ClO_4)_3$ into deionized water at a concentration of 10^{-3} M. Typically, the sample was immersed in the oxidant solution for 30−40 min. Ellipsometry data show that the thickness of the films did not change while the samples were immersed in the solution of the oxidant.

NL035099X